JOURNAL OF Applied Polymer SCIENCE

Improvement in physical and electrical properties of poly(vinyl alcohol) hydrogel conductive polymer composites

Winatthakan Phuchaduek,[1] Tongsai Jamnongkan,[2] Ubolluk Rattanasak,[1] Siridech Boonsang,[3] Supranee Kaewpirom[1]

[1]Department of Chemistry and Center of Excellence for Innovation in Chemistry, Faculty of Science, Burapha University, Chonburi 20131, Thailand

[2]Department of Fundamental Science and Physical Education, Faculty of Science at Siracha, Kasetsart University, Chonburi 20230, Thailand

[3]Department of Electrical Engineering, Faculty of Engineering, King Mongkut's Institute of Technology Ladkrabang, Bangkok 10520, Thailand

Correspondence to: S. Kaewpirom (E-mail: kaewpiro@buu.ac.th)

ABSTRACT: With an aim to develop anti-electrostatic discharge materials based on biodegradable polymers, poly(vinyl alcohol) films composited with two different conductive fillers (carbon black and aluminium) at various fillers contents (20−60%wt), were manufactured using solvent-casting technique. The mechanical properties of such the films were investigated through tensile stress-strain tests. Wettability and morphology of the composite films were performed by water contact angle measurement and SEM, respectively. Young's modulus of the composite films can be increased with the addition of conductive fillers. The surface of the composite films showed non-homogeneous appearance, in which the phase boundary within the composites was clearly observed and the conductive fillers formed aggregation structure at high filler concentration. In addition, the composite films exhibited better hydrophobicity when higher conductive filler content was added. TGA results suggested that both carbon black and aluminum have proven their efficiency to enhance thermal stability of poly(vinyl alcohol). Investigation of cross-cut adhesion performance of the prepared composite films revealed that carbon black-filled composites exhibited excellent adhesion strength. The effect of conductive filler content on surface resistivity of the composite films was also examined. The experimental results confirmed that both the fillers used in this study can improve the electrical conductivity of poly(vinyl alcohol) hydrogel. The surface resistivity of the composite films was reduced by several orders of magnitude when the filler of its critical concentration was applied. © 2015 Wiley Periodicals, Inc. J. Appl. Polym. Sci. **2015**, *132*, 42234.

KEYWORDS: composites; conducting polymers; morphology

Received 28 November 2014; accepted 15 March 2015
DOI: 10.1002/app.42234

INTRODUCTION

Recently, inorganic or metal particle based composites with polymer are one of the main focus points of research due to their technological applications.[1] Particularly, conducting polymer has received attention for several decades. There are several researchers who have proposed new technology for producing conducting polymers in order to apply in electronic devices.[2–4] Although conducting polymers are versatile materials, the majority of conducting polymers has low solubility in solvent, which makes difficulty in processing them. Several research groups have reported several techniques for producing conducting polymers, for examples, thermomechanical processing, blending, and compositing with other polymers or inorganic materials.[5–7]

In this regards, poly(vinyl alcohol), PVA, one of the biocompatible and biodegradable polymers, is especially attractive and has been successfully utilized as polymer matrix in conducting composite film fabrication.[8] PVA possesses good chemical resistance, thermal stability, high dielectric strength, and good charge storage capacity.[9,10] In addition, PVA has a crucial factor enhancing its suitability for film processing by solvent casting method. Its regular linear structure with a large number of hydroxyls on the molecular chain indicates excellent hydrophilicity. Therefore, it shows high water permeability and also dissolves easily in water.[11] Besides, it's well known that the dielectric permittivity of PVA is extraordinarily low. Thus, enhancement of the dielectric permittivity of the PVA-based composite materials while maintaining their mechanical performance is important for many technological applications. In recent years, some researchers have successfully produced conducting composite film based on PVA with inorganic materials such as PVA/grapheme,[12] PVA/gold nanoparticles,[13] and PVA/ZnO.[14]

Among the materials used for technological applications, carbon black (CB) has recently attracted attention due to its numerous desirable properties, such as good electrical conductivity, low cost, and good thermal and chemical stability.[15] Aluminum (Al) is one of the interesting commercial materials, used for compositing with common polymers in order to improve the electrical and thermal conductivity of such polymers.[16] Recently, Strzelec and Pospiech[17] reported the successful production of conducting composite film using polythiourethane-cured epoxy resin and aluminum.

To our knowledge, although several studies reported the preparation and properties of nanocomposite films, there was a few that reported on the preparation and properties of PVA/inorganic composite film. In this study, we aimed to develop biodegradable conducting composite films from PVA hydrogel compositing with CB or Al using solution-casting technique. The key objective of applying this method was to optimize the application properties with regard to the processability and cost. Morphology of prepared composite films was investigated using a scanning electron microscope (SEM). Mechanical strength and thermal stability were characterized by tensile testing and thermo gravimetric analysis (TGA), respectively. Hydrophilicity and adhesion strength of the composite films were also studied. Finally, to understand the electrostatic discharge (ESD) properties of these materials, surface resistivity of the prepared composite films was examined as a function of conductive filler content.

EXPERIMENTAL

Materials

PVA, M_w = 85,000–124,000 g/mol, and 3-aminopropyltriethoxysilane (APS) were purchased from Sigma-Aldrich (Germany). Glutaraldehyde (1.2% w/v) was obtained from Fluka (Switzerland). Two different types of conductive fillers were used in this study. Carbon black (CB), with the averaged particles size of 49 μm, was purchased from S.D. Fine-Chem (India). Aluminum powder (Al), with the averaged particle size of 26 μm, was received from Himedia (Germany). All the chemicals were analytical grade and used as received without any further purification.

Silanization

In order to provide bonding sites for the polymer composite to chemically bind to a glass surface, a glass slide was treated with APS coupling agent. Prior to silanization process, a glass slide was cleaned using a general glass cleaning protocol: immersion in 2.5*M* NaOH solution for 24 h, sonication in H_2O for 10 min, immersion in 0.1*M* HCl for 15 min, sonication in H_2O for 10 min and, finally, immersion in methanol for 5 min. Silanization was performed by dip-coating the cleaned glass slide in 1%v/v aqueous solution of APS for 15 min. Post-treatment steps included shaking in methanol for 5 min, followed by rinsing with H_2O. The coated slide was baked at 80°C for 40 min in a hot air oven and stored in a vacuum desiccator.

Preparation of Composite Films

A PVA solution with a concentration of 10% w/v was prepared by dissolving PVA in deionized water at 90°C under stirring for 2 h. To prepare PVA/CB composite, 10 mL of PVA solution was mixed with the appropriate amount of CB (20, 30, 40, 50, and 60%wt). Then 2.8 mL of crosslinking solution, prepared from 50%w/v methanol (the quencher), 10%w/v acetic acid (the pH controller), 1.20%w/v glutaraldehyde, and 10%w/v sulfuric acid (the catalyst), with solution volume ratio of 3 : 2 : 1 : 1, was added into the mixture under constant stirring for 15 min, in order to obtain a uniform distribution of the filler. In this study, the composite films were prepared by two different methods. One: the mixture was poured into a Petri dish, with the diameter of 10 cm, and kept in a hot air oven at 50°C for 12 h, followed by drying in a vacuum oven at 40°C for 24 h. By using this method, a dried film with the thickness of 100 μm was obtained. The other: the mixture was coated on a silanized glass slide using a bar-coater (K Hand coater, RK Printcoat Instruments, UK) and then cured in a hot air oven at 50°C for 12 h, followed by drying in a vacuum oven at 40°C for 24 h. The composite film with the thickness of 50 μm was obtained.

PVA/Al composites were also prepared. The appropriate amount of Al was used and the same procedure, used for PVA/CB preparation, was followed.

SEM Measurement

The surface morphology of composite films was investigated using scanning electron microscopy (SEM). A dried film was mounted on a metal stub using a double-sided adhesive carbon tape and was coated with gold. SEM micrographs of the composite films were recorded using a LEO-1450VP SEM.

Mechanical Properties

Mechanical properties of the composite films were performed according to ASTM D638 on a tensile tester (Testometric, Micro 350), with a 50 N load cell equipped with tensile grips. The composite films were cut into 5-mm-wide and 50-mm-long strips. Grip separation was set at 25 mm, and a cross-head speed was 500 mm min^{-1}. Tensile strength, Young's modulus, and elongation at break (%*E*) were evaluated. The tests were carried out at 23°C and 55% RH. At least 10 specimens were measured and the averaged values were taken.

Thermo Gravimetric Analysis (TGA)

Thermal stability behavior of the composite films was revealed using a TGA 7HT thermogravimetric analyzer. The sample (4−6 mg) was placed in a stainless pan and then heated from 50 to 700°C at a heating rate of 10°C min^{-1} under nitrogen atmosphere.

Contact Angle Measurement

Water contact angle was measured after a DI water droplet was set on the composite film surface and the side view pictures of the droplet were taken. Since the film's surface roughness increased with increasing filler loading content, great cautions were made on the measurements, in order to reduce the influence of air-gaps. In our experiment, a drop of water was suspended from a needle before the film surface was slowly moved into contact with such the pendant drop. Each reported contact angle was the mean value of at least five measurements, taken at different positions on the composite films.

Adhesion Strength

Cross-cut adhesion of the composite films was carried out according to ASTM D-3359-97. Square boxes of 1 mm^2 were made on a 1 cm × 1 cm square of the test specimen. The boxes

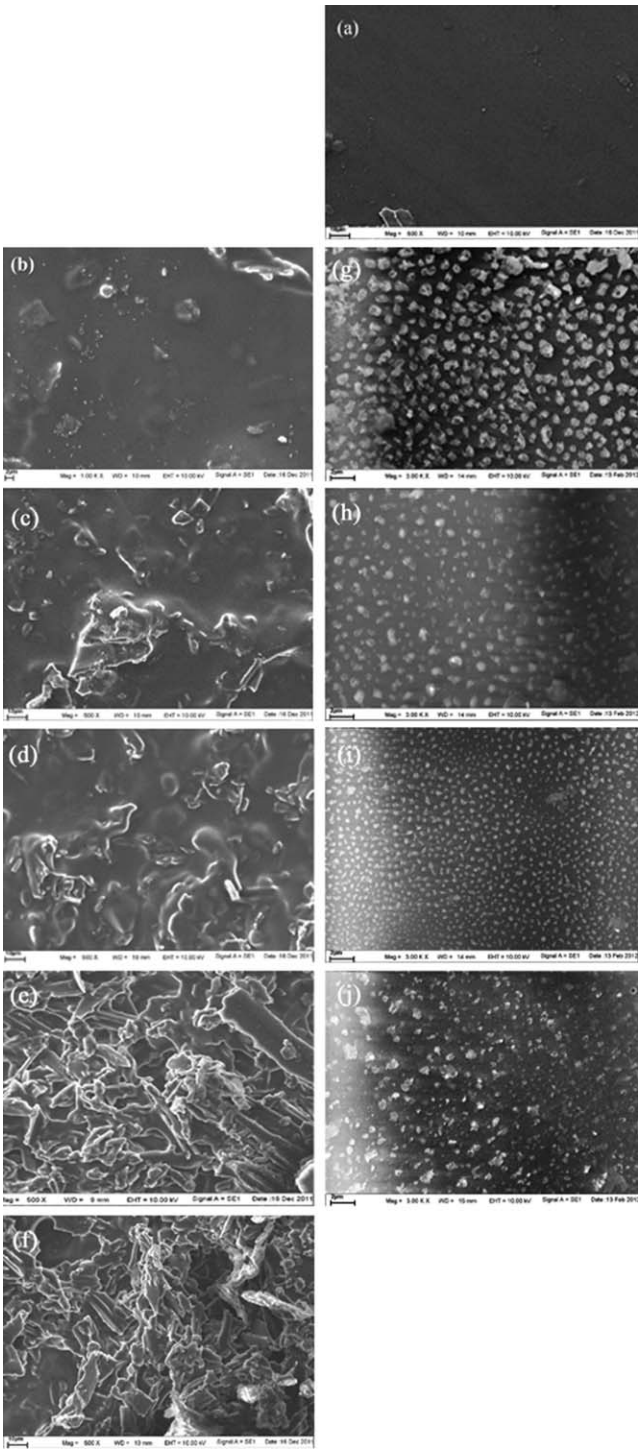

Figure 1. SEM images of PVA film (a) and PVA/conductive filler composite films with 20, 30, 40, 50, and 60% filler content: PVA/CB (b−f) and PVA/Al (g−j).

were covered by 3M^{TM} adhesive tape. The tape was then peeled off and the number of boxes removed from the glass surface was counted to check the adhesion strength of the films.

Electrical Property Measurement

The electrical conductivity of composite films was measured using a four-point probe digital multimeter (Agilent 34410A). The experimental procedure was as follows. Two copper electrodes were pressed on both sides of the composite film at the distance of ∼1.7 cm from each other. Two probes were placed between the copper electrodes at the distance of ∼1.5 cm from each other. The surface resistivity of the composite films was carried out according to ASTM D257-90 and was calculated using the equation:

$$\rho_s = R_s \frac{P}{g} \quad ; \quad P = 2(a + b + 2g) \tag{1}$$

where, R_s is the surface resistance (ohm), P is the effective perimeter of the guarded electrode for the particular arrangement (cm), g is distance between guarded electrode and ring electrode (cm), and a, b are the lengths of the sides of rectangular electrodes (cm).

RESULTS AND DISCUSSION

Scanning Electron Microscopy

The surface morphology of PVA film, PVA/CB- and PVA/Al-composite films are shown in Figure 1. Obviously, the results showed that the surface morphology dependened on both type and content of the conductive fillers. PVA film surface showed smooth and homogeneous appearance [Figure 2(a)]. On the other hand, the surface of all the composite films showed non-homogeneous appearance. The conductive fillers clearly displayed phase boundaries within PVA matrix, especially at high loading content, as seen in Figure 2(b–j). This behavior resulted from the poor polymer-conductive filler interaction, owning to weakly bonding interaction between the iorganic compound (conductive fillers) and organic compound (PVA). Hence, phase boundary within the composite films occured, and the conductive fillers likely formed aggregation structure.

Mechanical Properties

Figure 2 represents the representative tensile stress-strain curves of PVA/CB composites with selected CB concentrations (a), and tensile strength (b), Young's modulus (c), and elongation at break (d) of PVA/CB and PVA/Al composite films as a function of conductive filler content.

It was found that tensile strength of all the composite films significantly decreased with increasing conductive filler content. At 20%wt of conductive fillers, tensile strength of the composites decreased up to ∼83% and 38% for PVA/CB and PVA/Al, respectively, when compared with the neat PVA film [Figure 2(b)]. This was possibly due to the poor interfacial bonding and the presence of filler agglomeration.[18] In addition, the weak bonding between particles of conductive fillers and PVA obstructed the stress propagation and caused the tensile strength to decrease with the increase in conductive filler content. These are in accordance with prior results reported by Karnani *et al.*,[19] Oksman and Clemons,[20] and George *et al.*,[21] More relevantly, Wu *et al.*,[22] proposed that the non-homogeneity between the organic and inorganic phases became more serious when the inorganic filler content increased. Such the nonhomogeneity, therefore, deteriorated the mechanical strength of the composite films. Interestingly, the tensile strength of the composites slightly increased with increasing CB and Al above 50%wt and 40% %wt, respectively. Such the concentrations were consistent

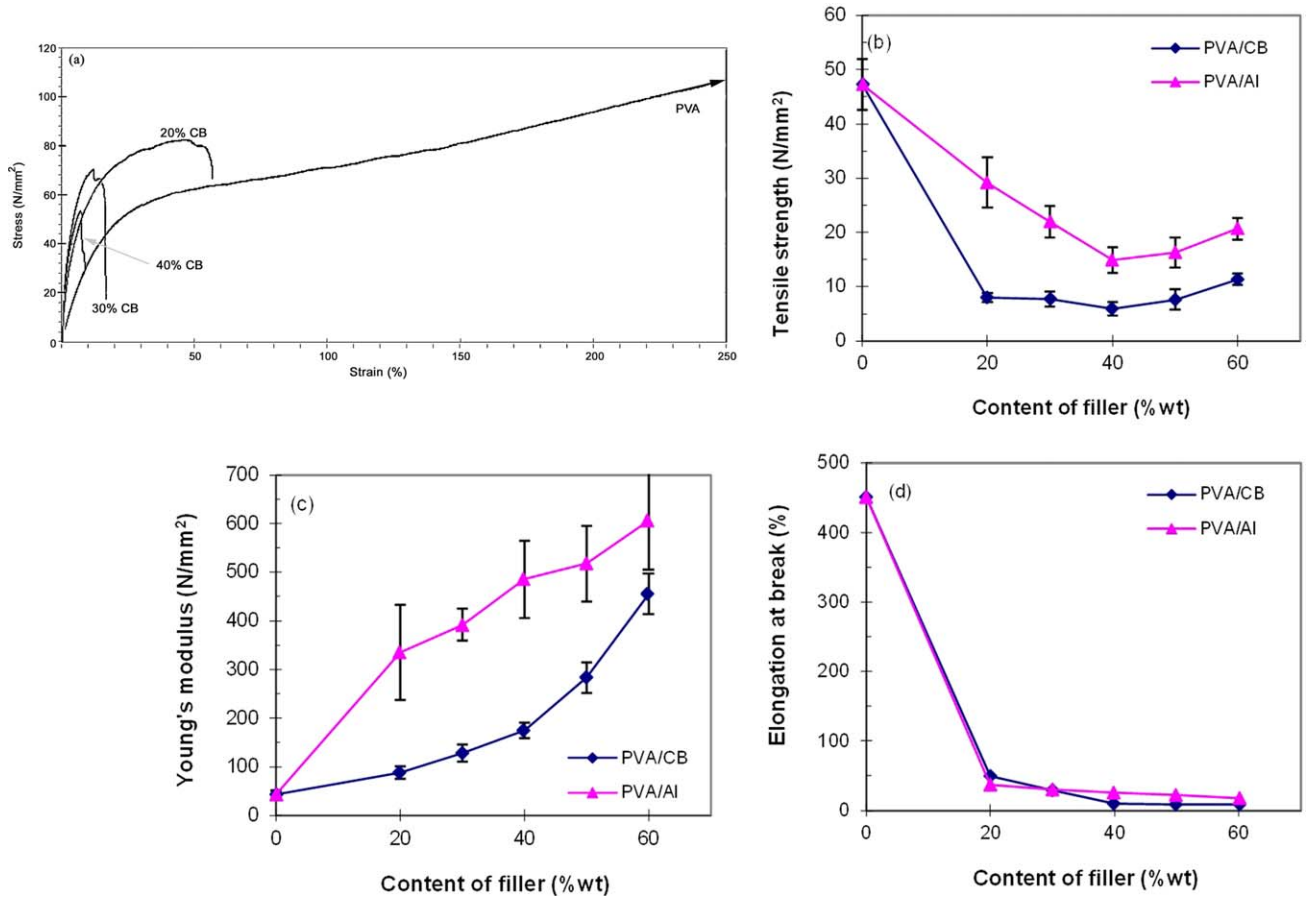

Figure 2. Representative tensile stress−strain curves of PVA/CB composites with selected CB concentrations (a), and tensile strength (b), Young's modulus (c), and elongation at break (d) of composite films against the conductive filler content. [Color figure can be viewed in the online issue, which is available at wileyonlinelibrary.com.]

with the percolation threshold of PVA/CB and PVA/Al, respectively (as will be discussed in Electrical Conductivity). Hence, the continuous conducting networks of the fillers within the composites were formed and the percolation threshold was met (as seen in SEM micrographs). This was responsible for the increase in the tensile strength. Beyond these concentrations, the number of conducting network increased with increasing filler content. As a result, the tensile strength of the composites increased.

Figure 2(c) shows the effect of conductive filler content on Young's modulus of PVA/CB, and PVA/Al composite films. As expected, the value of Young's modulus increased with the increase in conductive filler content. With high content of fillers (>30%wt of CB and >20%wt of Al), the Young's modulus extremely increased. Additionally, at a given filler concentration, it was found that the Young's modulus value for PVA/Al composite film was higher than that for PVA/CB. This is possibly due to the effect of particle size of the conductive fillers. It's well known that smaller particles can interact greater than larger ones, which is in good agreement with previous studies.[23–25]

The increase in Young's modulus of the composites when the filler content increased was believed to derive from both the shape of the inhomogeneity and the filler orientation; those are roughly proportional to their volume fraction in the composites. According to the Hashin-Shtrikman model,[26] the upper and lower bound moduli of a composite without any specific morphology except one phase is continuous and the other is discontinuous can be predicted by the equation:

$$G_1\frac{\upsilon_1 G_1+(\alpha_1+\upsilon_2)G_2}{(1+\alpha_2\upsilon_2.)G_1+\alpha_1\upsilon_1 G_2}<G_c<G_2\frac{\upsilon_2 G_2+(\alpha_2+\upsilon_1)G_1}{(1+\alpha_1\upsilon_1)G_2+\alpha_2\upsilon_2 G_1} \quad (2)$$

Davies[26] also showed that the modulus of a dual phase continuity model was raised to the one-fifth power:

$$G_c^{1/5}=\upsilon_1 G_1^{1/5}+\upsilon_2 G_2^{1/5} \quad (3)$$

Where G_c, G_1, G_2 represent the modulus of the composite and the constituents 1 and 2, where $G_2 > G_1$, and υ_1 and υ_2 are the volume fractions of the constituents 1 and 2, respectively, and $\alpha = 2(4-5\nu)/(7-5\nu)$, a function of Poisson's ratio. In Figure 2(b), the Young's modulus of PVA/CB composites increased exponentially with the increase in CB content. This corresponds with the model proposed by Hashin-Shtrikman (the lower bound modulus). Contrariwise, PVA/Al composites exhibited the increased in Young's modulus as Al content increased. Such behavior followed Davies model.

Figure 2(d) depicts the effect of conductive filler types and content on the elongation at break of the prepared composite films. The PVA film, without conductive fillers, showed the highest elongation at break (~450%). As expected for all the samples,

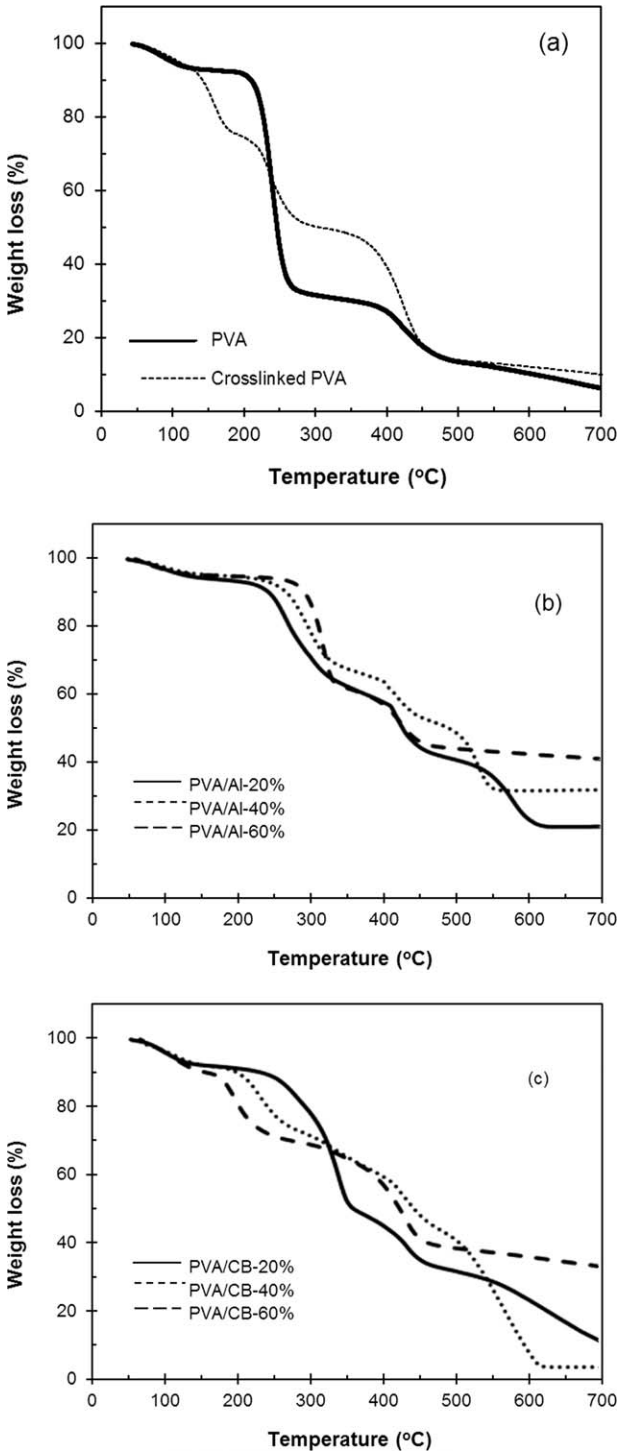

Figure 3. TGA thermograms of PVA and crosslinked PVA (a), PVA/Al (b), and PVA/CB (c) composite films.

the elongation at break decreased sharply (approximately up to 88% reduction) with 20%wt of conductive fillers. This is possibly due to stiffening property of the PVA composite films caused by intermolecular interaction between PVA chains and conductive fillers particles. Additionally, the reduction of elongation at break was also affected greatly by the hard filler content. The higher the conductive filler content within the PVA composite films structure, the lower the elongation at break was. The reason for these is the decrease in molecular mobility due to extensive formation of physical bonding between the particles of conductive fillers and the PVA chains that stiffen the matrix.[23] Moreover, type of conductive fillers also affected the elongation at break of composite films. At a given concentration, PVA/Al composite films showed higher elongation at break than PVA/CB composite films. This behavior was possibly caused by the effect of particle size of conductive fillers within polymer matrix, as discussed earlier.

Thermo Gravimetric Analysis (TGA)

Figure 3(a) shows TGA thermograms for PVA and crosslinked PVA films. PVA exhibited three-step degradation behavior, which is the same tendency as that reported by Chen *et al.*[27] Initial loss ($T_{d,1}$) in mass was due to moisture vaporization. The majority of the weight loss ($T_{d,2}$) taking place between 200 and 300°C was due to the thermal degradation of PVA molecules. Further weight loss ($T_{d,3}$) between 390 and 420°C was possibly due to a breakdown of the PVA backbone in the molten state, that generated by-products such as ketone compounds. The results were in good accordance with the results presented by Holland and Hay.[28] Besides, crosslinked PVA showed higher thermal stability than the neat PVA, owing to the chemical crosslinking within PVA structure.[27] The experimental data are presented in Table I.

In addition, we investigated the thermal stability of the composite films and the results are shown in Figure 3(b,c). As expected, all the samples displayed a gradual decrease in weight as the temperature increased from 50 to 700°C. A similar behavior was observed in TGA thermograms for all the composite films, wherein four different zones of thermal decomposition were observed. Figure 3(b) shows thermal stability patterns for PVA/Al composite films with different Al concentrations. Regardless of Al concentration, the $T_{d,1}$ observed below 100°C was caused by the evaporation of water. The $T_{d,2}$ exhibiting the degradation of PVA chains was found at 259, 287, and 312°C for PVA/Al composite films with 20, 40, and 60%wt of Al, respectively. The $T_{d,3}$ and $T_{d,4}$, found between 400 and 420°C, and above 500°C, respectively, indicated the thermal degradation related to the oxidation of Al.[29] As expected, the char residue increased with

Table I. Summary of the TGA Thermograms of PVA, PVA/Al, and PVA/CB Composite Films

Samples	$T_{d,1}$ (°C)	$T_{d,2}$ (°C)	$T_{d,3}$ (°C)	$T_{d,4}$ (°C)	Residue (%)
PVA	82	234	417	–	6.2
Crosslinked PVA	162	235	419	–	10.1
PVA/CB-20%	86	332	425	–	11.5
PVA/CB-40%	94	326	440	568	4.0
PVA/CB-60%	94	182	423	–	33.3
PVA/Al-20%	90	259	409	576	19.7
PVA/Al-40%	88	287	400	527	31.1
PVA/Al-60%	76	312	419	–	40

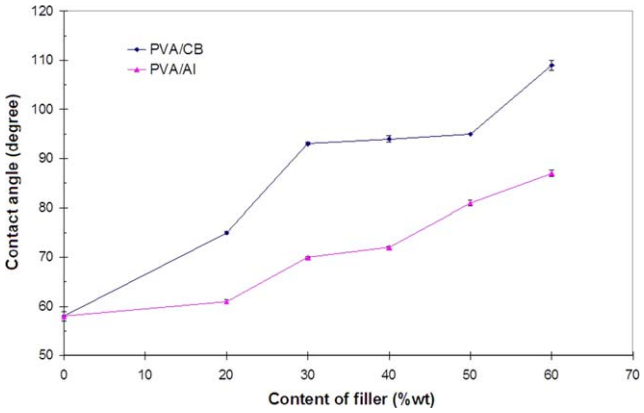

Figure 4. Water contact angle on the surfaces of PVA/CB and PVA/Al composites against the conductive filler content. [Color figure can be viewed in the online issue, which is available at wileyonlinelibrary.com.]

the increase in Al content. Therefore, the thermal stability of PVA composite films depended on Al concentration, as summarized in Table I. It's worth to conclude that Al has proven its efficiency in improving the thermal stability of PVA. Relevantly, Kuljanin *et al.*,[30] stated that the filler particles have a significant barrier effect to slow volatilization rate of composites during decomposition, which enhance the thermal stability of composites due to chain mobility restriction effects of polymer chains. Figure 3(c) shows the TGA thermograms of PVA/CB composite films, wherein the results exhibited the four-step degradation behavior as those of PVA/Al composite films. Regarding to the major thermal decomposition ($T_{d,2}$), the experimental results showed $T_{d,2}$ of 332, 326, and 182°C for PVA/CB composite films with 20, 40, and 60%wt of CB, respectively. The $T_{d,2}$ for PVA/CB composite films significantly decreased with the increase in CB concentration [Figure 3(c)]. This is in accordance with the results reported by Jakab and Blazso.[31] They investigated the effect of carbon black on the thermal decomposition of vinyl polymers (such as PMMA, PP, and PS). They stated that the concentration of CB in the composite films pointed to the importance of the physical contact between the carbon black and the polymer chains. It was also stated by Roy *et al.*[32] that CB consists of various functional groups such as carbonyl, phenols, lactones, aldehydes, ketones, quinines, and ethers on its surface. Oxidative degradation of PVA/CB, therefore, took place drastically as CB content increased. This leaded to the reduction of $T_{d,2}$. Hence, it can be concluded from the results in Figure 3 and Table I that thermal stability of the composite films depended not only on the conductive fillers loading content, but also on the type of conductive fillers.

Contact Angle Measurement

The wettability on the surface of composite films was measured by water contact angle. It's well known that if on a surface whose contact angle of water droplet is greater than 150°, it can be regarded as superhydrophobic.[33] Thus, a value of water contact angle can reflect the hydrophilic properties of the composite films. In this study, we carefully measured the water contact angle of the composite films in order to avoid the effect of air gaps that was possibly found on the rough composite film surface (as already described in Experimental). It was found that the hydrophobic property of PVA surface can be improved slightly by crosslinking reaction, as observed from contact angle values (53° and 58° for neat and crosslinked PVA, respectively). In addition, the water contact angle increased with increasing conductive filler content, as shown in Figure 4. In the figure, each value represents an average of five measurements with the standard deviation less than 1°. At a given conductive fillers concentration, PVA/CB shows higher water contact angle than that of PVA/Al composite films. This highly displayed that PVA/CB composite was more hydrophobic. Interestingly, the results are in good agreement with the results obtained from SEM micrographs. In the micrographs, although CB particles were well dispersed on the composite film surfaces, the agglomeration of CB particles was obviously observed, especially at high CB content. On the other hand, the agglomeration of Al particles was not observed in PVA/Al composite surface, even at high Al content. Therefore, the agglomeration of the filler particles on the film surface was responsible for the increase in the water contact angle of the composites.

In addition, water contact angle of composites was nearly constant when the filler concentrations were in the range 30−50% for PVA/CB and 30−40% for PVA/Al composites, respectively. Such the ranges were corresponded to the ranges that abrupt transitions in surface resistivity of the composites were observed (see the explanation in Electrical Conductivity). This also confirmed the aggregation of the majority of CB particles, forming continuous chains, or networks. After these critical ranges, the water contact angle of the composites increased further as the filler content increased, owing to the increase in the filler particle coverage on the composite surface.

The increment of water contact angle as the surface roughness increased can be explained by Cassie model.[34] When a water droplet drops on the surface, air and the solid rough surface forms a composite surface, according to the Cassie equation:

$$\cos\theta_c = f_s \cos\theta_s + f_v \cos\theta_v \quad (4)$$

where θ_c is the apparent water contact angle, and f_s and f_v are the area fractions of the solid and air on the surface, respectively. Since $f_s + f_v = 1$, $\theta_s = \theta$, $\theta_v = 180°$, eq. (4) can be written as eq. (3):

$$\cos\theta_c = f_s(\cos\theta_s + 1) - 1 \quad (5)$$

In our study, the increase in filler content enhanced the surface roughness of the composites. Therefore, acting as eq. (5), the water contact angle also increased accordingly.

Cross-Cut Adhesion

The surface adhesion of the composites was performed on a glass slide substrate, using cross-cut adhesion technique. The adhesion performance of the prepared composite films, at different concentrations of conductive fillers, is shown in Table II.

In Table II, cross-cut adhesion results were based on a 0 to 5 scale, where 5 indicates excellent adhesion and 0 shows full delamination. It was found that there was no square specimen pulled off by the adhesive tape for PVA/CB composite films. This indicates that such the composite exhibited extremely high

Table II. Cross-Cut Adhesion Performance of PVA/CB and PVA/Al Composite Films

Filler	Filler content (wt %)	Adhesion (cross-cut)[a]
CB	20	5
	30	5
	40	5
	50	5
	60	5
Al	20	2
	30	2
	40	1
	50	1
	60	0

[a] Numbers from 0 to 5 represent the increase of adhesive force.

adhesion strenghth on glass-slide surface. It was believed that the strong adhesion between the composite film and the silanized glass substrate was due to the formation of hydrogen bondings between the OH groups in the composite and the NH_2 groups on the surface modified glass substrate. On the other hand, the adhesion strenght of PVA/Al composite films decreased with the increase in Al content, indicating the poorer adhesion performance, compared with PVA/CB composite. This was possibly due to either the decrease in adhesion strength between Al particles or the increase in brittleness of the composites as PVA content decreased. Conclusively, PVA/CB composites can be potentially used as coatings for silanized glass surface, while PVA/Al composites are unsuitable for use as coatings, but may be potentially used as other forms of EDS materials.

Electrical Conductivity

In natural state, almost all commercial plastics are electrical insulators. The electrical charges deposited on a polymer surface are long-lived. This causes damage to electronics that come near or into contact with it. Making plastics to be either electrically static dissipative or electrically conductive, hence, is the way to reduced such damage. It's well known that low value of surface resistivity reflects good electrical conductivity of materials. Therefore, it's worthwhile to further examine the effect of the conductive fillers on the electrical conductivity of the prepared composite films. The effect of conductive filler content on surface resistivity of the prepared composite films is depicted in Figure 5. In the figure, the surface resistivity of PVA considerably decreased with the increase in conductive filler loading content. Obviously, the surface resistivity of the PVA/CB composite films decreased approximately two orders of magnitude when the CB-content increased from 20 to 60%wt. Such the decrease in surface resistivity was probably due to the generation of more conductive paths of the fillers network, as also stated by Subramniam *et al.*[35] It can also be clearly seen in Figure 5 that the resistivity of the composites can be reduced constantly by the addition of conductive fillers until it dropped suddenly when the conductive filler content reached a critical concentration. A significant drop in resistivity of PVA/CB composites was observed beyond 40%wt filler content. In this region a relatively small increase in filler content produced larger decrease in surface resistivity. Further increase in filler content beyond the critical concentration region caused marginal change in the surface resistivity of the composites. Thus, for PVA/CB composites, there was a marginal change in the surface resistivity at 40%wt filler content. Then the resistivity showed a sudden drop, giving rise to a very sharp transition from a high to a low resistance at 50%wt filler content. As a consequence, we can conclude that the abrupt transition in surface resistivity of PVA/CB composites occurred in the concentration range 40−50%wt. Such the sudden drop of surface resistivity in the composites with higher proportions of conductive filler was consistent with the aggregation of filler particles in the composites, as also seen from SEM images [Figure 2(d,e)]. Within this concentration range of fillers, the composites behaved like a semi-conducting material suitable for ESD applications. This point is called percolation threshold and represents that there is enough conductive filler present to make a continuous conducting networks within the composites. Beyond such critical concentration, the rate of decrease in resistivity occurred at a much slower rate. This was because, in this region, the increase in filler concentration simply signified an increase in the number of conductive network. The phenomenon may be visualized by considering that a continuous conducting wire (constituting an interconnecting chain) was formed throughout the insulating matrix at the critical concentration and further increase in the filler content simply increased the diameter of that conducting wire.[36] Figure 6 gives a simplified view of the percolation threshold. At low filler content, the filler particles act like conductive islands in the sea of insulating polymer matrix. As the filler content increases, the conductive particles become crowded and are more likely to come into contact with each other. Finally, as enough amount of conductive filler present, a majority of filler particles are in contact with neighbors, thereby forming a continuous network. Electrical charges, therefore, can pass through the composite via the networks. As mentioned above, the conductive networks in PVA/CB composites can be formed via the contacts of CB particles, hence, the conductive mechanism underlying these materials was contact conduction.[37]

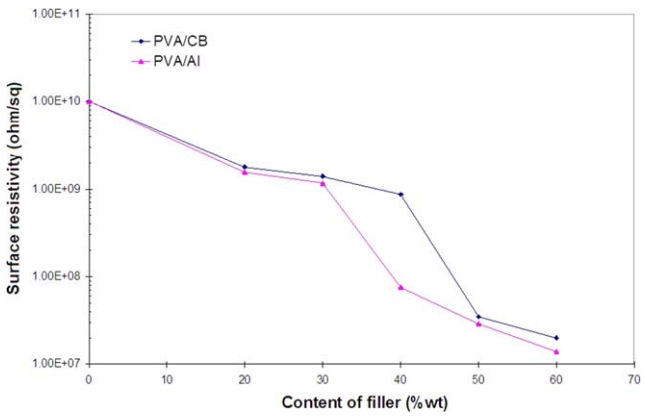

Figure 5. Surface resistivity of the prepared composites against the conductive filler content. [Color figure can be viewed in the online issue, which is available at wileyonlinelibrary.com.]

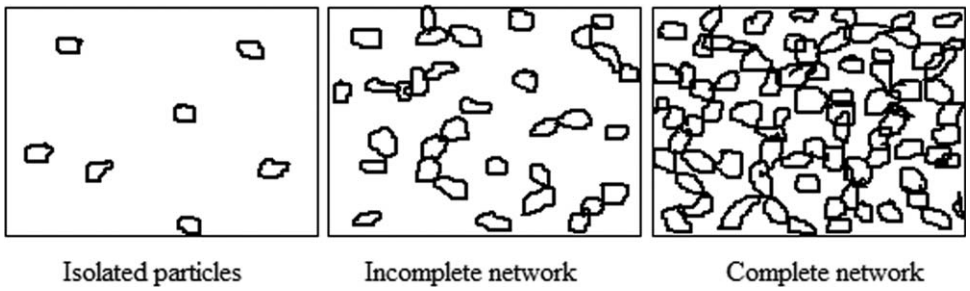

Figure 6. Proposed morphology of conducting network forming.

Similar behavior was also observed for PVA/Al composites. Here, the abrupt transition of the surface resistivity occurred in the concentration range 30−40%wt. In comparison with PVA/CB composites, the loading for such the onset of transition was lower. According to Rosner,[38] the shape of the filler particle plays an important role at what filler content percolation occurs. As seen from SEM micrographs [Figure 1(h,i)], Al particles displayed angular morphology with low to medium sphericity. At percolation threshold, although the surface resistivity of the composite reduced greatly, the Al particles were not in contact with their nearest neighbors. This implied the existence of the tunneling conduction that was governed by the charge carries between highly conducting regions (Al particles) that surrounded by insulating PVA matrix.[39] The close proximity of the Al particles enabled the tunneling of electrons to occur from one particle to another.[40,41]

Many companies have developed ESD control films those commercially available (Table III).

In summary, the surface resistivity of the proposed composites is in the ranges of those reported by the manufacturers. However, their mechanical properties, e.g., elongation, tensile modulus, and tensile strength, are lower than those of some commercial ESD films, available presently.

CONCLUSIONS

Conducting composite films based on PVA were successfully prepared by film casting technique. This provided the possibility of producing new conducting composite films from PVA using CB and Al as conductive fillers. The experimental results exhibited that the conductive filler particles, at low concentrations, well dispersed in the PVA matrix, and the composites displayed obvious phase boundaries when the conductive filler content increased. Although the Young's modulus of the composites increased with increasing filler content, the tensile strength and elongation at break of the composites reduced dramatically due to their poor interfacial bonding and the presence of filler agglomeration. The PVA/CB composite films displayed excellent adhesion on the glass substrate, while PVA/Al composite film exhibited poor adhesion strength. Thermal stability of the composite films can be improved by the addition of conductive fillers. The wettability of the conducting composite films decreased with the increase in conductive fillers concentration, which reflects the enhanced hydophobic property of composite films.

Table III. Some Properties of Commercially Available ESD Control Films

Name	Polymer matrix	Thickness (mm)	Surface resistivity (Ohm/sq)	Tensile modulus (MPa)	Tensile strength (MPa)	Elongation (%)	Manufacturer
Wescorp ESD Tape	[a]	0.05	10^{10}–10^{11}	[a]	0.17	25	Desco Industries Inc., CA.
TMF-300	Polyester	4	10^{6}–10^{8}	[a]	165[c]	200[c]	C.C.Steven and Associates, CA.
ABF-300	Polyester	4	10^{6}–10^{8}	[a]	172	a	C.C.Steven and Associates, CA.
CABELEC® 6141	Polycarbonate	[a]	10^{5}	2,168[b]	47	24	Cabot Coporation, Switzerland.
CABELEC® 4918	LDPE	0.05–0.1	5.1×10^{3}	A	20.5[c]	580[c]	Cabot Coporation, Switzerland.
PVA/CB(40-50%)	PVA	0.05-0.1	8.7×10^{8} to 2.9×10^{7}	175–283	5.9–7.6	9.2–8.4	This study
PVA/Al(30-40%)	PVA	0.05-0.1	1.2×10^{9} to 7.6×10^{7}	392–486	21.9–14.9	30–25	This study

[a] No reports.
[b] Flexural modulus.
[c] Machine direction.

In addition, this behavior was also dependent on the type of conductive fillers. As expected, the surface resistivity of the composite films was observed to drop by several orders of magnitude at a critical filler concentration region. The contact conduction and tunneling conduction were the models for electrical conduction in PVA/CB and PVA/Al composites, respectively. This is shown to be consistent with the composite morphologies.

ACKNOWLEDGMENTS

Financial supports from the Center of Excellence for Innovation in Chemistry (PERCH-CIC), Commission on Higher Education, Ministry of Education is gratefully acknowledged.

REFERENCES

1. de Barros, R. A.; Martins, C. R.; de Azevedo, W. M. *Synth. Met.* **2005**, *155*, 35.
2. Sirringhaus, H.; Kawase, T.; Friend, R. H.; Shimoda, T.; Inbasekaran, M.; Wu, W.; Woo, E. P. *Science* **2000**, *290*, 2123.
3. Kawase, T.; Sirringhaus, H.; Friend, R. H.; Shimoda, T. *Adv. Mater.* **2001**, *13*, 1601.
4. Balamurugan, A.; Ho, K. C.; Chen, S. M. *Synthetic Met.* **2009**, *159*, 2544.
5. Laska, J.; Izak, P.; Pron, A. *J. Appl. Polym. Sci.* **1996**, *61*, 1339.
6. Pud, A.; Ogurtsov, N.; Korzhenko, A.; Shapoval, G. *Prog. Polym. Sci.* **2003**, *28*, 1701.
7. Martins, C. R.; De Paoli, M. A. *Eur. Polym. J.* **2005**, *41*, 2867.
8. Makled, M. H.; Sheha, E.; Shanap, T. S.; El-Mansy, M. K. *J. Adv. Res.* **2013**, *4*, 531.
9. Ding, B.; Kim, H. Y.; Lee, S. C.; Shao, C. L.; Lee, D. R.; Park, S. J.; Kwag, G. B.; Choi, K. J. *J. Polym. Sci. Part B: Polym. Phys.* **2002**, *40*, 1261.
10. Mohamed, S. A.; Al-Ghamdi, A. A.; Sharma, G. D.; El Mansy, M. K. *J. Adv. Res.* **2014**, *5*, 79.
11. Jamnongkan, T.; Wattanakornsiri, A.; Wachirawongsakorn, P.; Kaewpirom, S. *Polym. Bull.* **2014**, *71*, 1081.
12. Mitra, S.; Mondal, O.; Saha, D. R.; Datta, A.; Banerjee, S.; Chakravorty, D. *J. Phys. Chem. C* **2011**, *115*, 14285.
13. Uddin, M. J.; Chaudhuri, B.; Pramanik, K.; Middy, T. R.; Chaudhuri, B. *Mater. Sci. Eng. B-Solid* **2012**, *177*, 1741.
14. Roy, A. S.; Gupta, S.; Sindhu, S.; Parveen, A.; Ramamurthy, P. C. *Compos. Part B-Eng.* **2013**, *47*, 314.
15. Xue, P. F.; Wang, J. B.; Bao, Y. B.; Li, Q. Y.; Wu, C. F. *Chinese J. Polym. Sci.* **2012**, *30*, 652.
16. Rufino, B.; Coulet, M. V.; Bouchet, R.; Isnard, O.; Denoyel, R. *Acta Mater.* **2010**, *58*, 4224.
17. Strzelec, K.; Pospiech, P. *Prog. Org. Coat.* **2008**, *63*, 133.
18. Kord, B. *World Appl. Sci. J.* **2011**, *13*, 171.
19. Karnani, R.; Krishnan, M.; Narayan, R. *Polym. Eng. Sci.* **1997**, *37*, 476.
20. Oksman, K.; Clemons, C. *J. Appl. Polym. Sci.* **1998**, *67*, 1503.
21. George, J.; Sreekala, M. S.; Thomas, S. *Polym. Eng. Sci.* **2001**, *41*, 1471.
22. Wu, Y.; Wu, C.; Li, Y.; Xu, T.; Fu, Y. *J. Membr. Sci.* **2010**, *350*, 322.
23. Sau, K. P.; Chaki, T. K.; Khastgir, D. *J. Appl. Polym. Sci.* **1999**, *71*, 887.
24. Oui, P. S.; Rakdee, C.; Thanmathorn, P. *J. Appl. Polym. Sci.* **2002**, *83*, 2485.
25. Ahmad, A.; Mohd, D. H.; Abdullah, I. *Iran. Polym. J.* **2004**, *13*, 173.
26. Sperling, L. H. In Polymeric Multicomponent Materials An Introduction; Wiley: New York, **1997**; Chapter *2*, p 37.
27. Chen, C. H.; Wang, F. Y.; Mao, C. F.; Liao, W. T.; Hsieh, C. D. *Int. J. Biol. Macromol.* **2008**, *43*, 37.
28. Holland, B. J.; Hay, J. N. *Polymers* **2001**, *42*, 6775.
29. Trunov, M. A.; Schoenitz, M.; Zhu, X.; Dreizin, E. L. *Combust. Flame.* **2005**, *140*, 310.
30. Kuljanin, J.; Marinović-Cincovic, M.; Stojanovic, Z.; Krklješ, A.; Abazovic, N. D.; Comor, M. I. *Polym. Degrad. Stab.* **2009**, *94*, 891.
31. Jakab, E.; Blazso, M. *J. Anal. Appl. Pyrol.* **2002**, *64*, 263.
32. Roy, N.; Sengupta, R.; Bhowmick, A. K. *Prog. Polym. Sci.* **2012**, *37*, 781.
33. Liu, F.; Wang, S.; Zhang, M.; Ma, M.; Wang, C.; Li, J. *Appl. Surf. Sci.* **2013**, *280*, 686.
34. Wang, H.; Dai, D.; Wu, X. *Appl. Surf. Sci.* **2008**, *254*, 5599.
35. Subramaniam, K.; Das, A.; Simon, F.; Heinrich, G. *Eur. Polym. J.* **2013**, *49*, 345.
36. Pramanik, P. K.; Khastgi, D.; Saha, T. N. *Composites* **1992**, *23*, 183.
37. Zhang, Y.-C.; Dai, K.; Tang, J.-H.; Ji, X.; Li, Z.-M. *Mater. Lett.* **2010**, *64*, 1430.
38. Rosner, R. B. Electrical Overstress/Electrostatic Discharge Symposium Proceedings, Anaheim, CA, 26–28 September 2000, pp 121–131.
39. Sheng, P. *Phys. Rev. B.* **1980**, *21*, 2180.
40. Mitra, S.; Banerjee, S.; Chakravorty, D. *J. Appl. Phys.* **2013**, *113*, 154314.
41. Krupka, J.; Strupinski, W. *Appl. Phys. Lett.* **2010**, *96*, 082101.